ELSEVIER

Surface Science 364 (1996) L617–L624

surface science

Surface Science Letters

Structure of the Be(11$\bar{2}$0) surface

J.B. Hannon[a,1], K. Pohl[b,*,2], P.J. Rous [c], E.W. Plummer [a,b]

[a] *Department of Physics and Astronomy, The University of Tennessee, Knoxville, TN 37996-1200, USA*
[b] *Solid State Division, Oak Ridge National Laboratory, Oak Ridge, TN 37831-6057, USA*
[c] *Department of Physics, University of Maryland, Baltimore County, Cantonville, MD 21228, USA*

Received 15 February 1996; accepted for publication 7 May 1996

Abstract

The equilibrium structure of the Be(11$\bar{2}$0) surface has been determined using LEED *I–V* analysis. This surface exhibits a stable (1 × 3) reconstruction over the range of temperatures investigated (100–720 K) where the surface starts to disorder. The equilibrium structure consists of a missing-row reconstruction in which every third surface chain of the bulk-terminated structure is absent. The experimentally determined structure is at odds with first-principles calculations, which favor a relaxed but unreconstructed bulk termination.

Keywords: Alkaline earth metals; Density functional calculations; Low energy electron diffraction; Low index single crystal surfaces; Surface relaxation and reconstruction

The electronic states and bond lengths at metal surfaces are, in general, not identical to those of the bulk because the coordination and symmetry of the surface is not bulk-like. Atoms at a surface relax in order to lower the energy of the crystal. In the simplest cases, the relaxation of the surface does not involve a change in the symmetry parallel to the surface (no reconstruction), allowing for a rather simple discussion of the physics: the charge spills out into the vacuum, and smoothes out the electronic surface corrugation [1], while new surface states can exist in gaps in the projected bulk band structure. Both effects can induce changes in the interlayer spacing. A more chemical understanding can be reached by considering a bond-order to bond-length correlation as given by Pauling [2]. When a surface is formed, the surface atoms decrease their coordination, which leads to a redistribution of the binding valence electrons in a fewer bonds. This effect can change the bond-length and often the layer separation. With modern experimental and theoretical techniques it is relatively easy to determine the electronic and structural properties of these simple, unreconstructed surfaces. The perception is that this problem is solved, because one finds a general agreement between theory and experiment. More importantly this agreement leads to a physical picture of the origin of effects such as the crystal-face dependence of the work function and interplanar spacing. Recently, this premise has been challenged [3–5]. Seitsonen et al. have used the three low index faces of Al to make the following point: experiment and

* Corresponding author. Fax: +1 423 5768135; e-mail: pohl@solid.ssd.ornl.gov

[1] Present address: IGV, Forschungszentrum Jülich GmbH, 52425 Jülich, Germany.

[2] On leave from the University of Pennsylvania.

PII S0039-6028(96)00797-2

theory agree on the order of the face-dependence of the work function, and on the trends in the interplanar relaxation, but neither are compatible with the intuitive picture of charge smoothing [1] or the effect of the smoothing upon the interplanar spacing in the Finnis–Heine model [6]. Feibelman [5] raised an even more serious issue when he compared the measured and calculated first interplanar relaxation for the close-packed surfaces of reactive transition metals. His comparison showed that the theory always predicted a considerably larger interplanar relaxation than that measured experimentally – on average four times bigger. Feibelman argues that this discrepancy could be caused by hydrogen contamination. The discrepancy may, however, be intrinsic to LDA or related technical problems associated with computations for transition metals.

Be is an s–p bonded metal, but the electronic structure does not resemble that of a free-electron metal: the calculated density of states of bulk Be shows a minimum near the Fermi energy, and the band structure exhibits band gaps at the zone boundary which are as large as 40% of the occupied-band width [7]. It serves as an intermediate material somewhere between the simplicity of Al and the complexity of the transition metals. The electronic and structural properties of the Be(0001) [7–10] and Be(10$\bar{1}$0) [11,12] surfaces have been measured and compared to theoretical calculations. In general, these surfaces fall into the category of simple metal surfaces because of the presence of an extremely high density of surface states at the Fermi energy. Here experiment and theory are in quite good agreement, with the one exception of the large (6%) interplanar expansion measured for Be(0001) [8] compared to the value of 2.7% calculated using LDA [13]. Unlike the close-packed (0001) surface, or the more open (10$\bar{1}$0) surface, we find that the equilibrium structure of the (11$\bar{2}$0) surface is reconstructed. Specifically, the surface undergoes a (1×3) missing-row (MR) reconstruction in which every third surface chain of atoms of the bulk-terminated structure is absent. The geometry of the surface is similar to that of the MR reconstructions which have been observed at the fcc (110) surfaces of Au [14], Pt [15] and Ir [16]. Here is a simple s–p bonded metal with a stable reconstruction that can be used to test the theory of surface reconstructions, without the complexity of d or f electrons.

For the Au(110) and Ag(110) surfaces, the first-principles calculations by Ho and Bohnen [18] have shown that the stability of the surface against reconstruction is related to the effectiveness of local d–d hybridization. For the case of the MR reconstruction at the Be(11$\bar{2}$0) surface, the mechanism must be different because Be possesses no occupied d-bands. The unusual bonding of bulk Be reflects the unique properties of the Be atom: the valence shell is closed and s-like. As a consequence, bonding between Be atoms requires promoting an electron from the s shell to the unoccupied p shell. The s–p excitation energy is so high (2.8 eV) that occupied p states contribute insignificantly to the binding of the Be dimer, which is bound essentially by van der Waals-strength forces [19]. However, in the maximally coordinated environment of the bulk, the energy of the p-derived states is insignificantly lowered. These states play an active role in the binding of the solid, which has a relatively high cohesive energy of 3.2 eV [17]. The close-packed (0001) surface is unreconstructed, but exhibits a large expansion of the first interlayer spacing [8,9]. The equilibrium structure of the low-density (10$\bar{1}$0) surface corresponds to the short termination [12].

We have determined the structure of the Be (11$\bar{2}$0) surface using low energy electron diffraction (LEED *I–V*), where we compared the measured intensity of the diffracted beams to that calculated using multiple scattering theory. This analysis complements earlier work based on a simple kinematic scattering model [20]. The kinematic analysis gives strong support for a surface structure based on periodic missing- or added-rows at the surface, but cannot be used to distinguish reliably between different missing-row models. The full dynamical calculations favor the single missing-row model over any of the trial structures considered, i.e. a (10$\bar{1}$0) microfacet model, and a single added-row model.

The calculation of the diffracted intensity was performed using standard multiple-scattering algorithms [21,22]. A maximum of 11 phase shifts, supplied by Müller and Heinz [23], were used to

describe the Be scattering potential. Intralayer scattering was treated exactly via matrix inversion and the layers were stacked using renormalized forward scattering [22]. Thermal vibrations were introduced by modifying the phase shifts using a Debye temperature converted into isotropic mean square displacements $\langle u^2 \rangle$ by evaluating the Debye integral [22]. In order to account for the different vibrational properties of the atoms at the surface and in the bulk, we optimized the Debye temperature of the top Be surface layer Θ_D^s, while fixing the bulk layers at the experimental value of $\Theta_D^b = 1400$ K [24] or $\langle u^2 \rangle^b = 0.0088$ Å^2. Attenuation of the incident and scattered electron beams was introduced via an energy-dependent imaginary part of the inner potential V_{0i}, modeled by the equation

$$V_{0i} = c\left(\frac{E - V_{0r}}{200\,\text{eV} - V_{0r}} \right)^{1/3},$$

where E is the electron energy. The constant c is a free parameter which is determined as part of the optimization. The real part of the inner potential $V_{0r} = a + bE$ was also optimized during the search procedure. Based on the described input, we calculated I–V spectra in the energy range from 50 to 450 eV in 2 eV steps for several thousand trial structures.

During the search for optimum agreement between experiment and calculation, both structural (atomic coordinates) and non-structural (i.e. V_{0i}, V_{0r} and Θ_D^s) parameters were varied. Agreement between the calculated and measured I–V curves was quantified using the Pendry R-factor R_P [25], which is sensitive to the peak position and the existence of small peaks in the spectra [25]. The set of parameters which correspond to the minimum value of R_P is taken to describe the most likely structure of the surface.

We have prepared several Be(11$\bar{2}$0) samples, which we cleaned in vacuum following the procedure described in Ref. [20]. The cleanliness was verified using Auger electron spectroscopy, the largest contaminants being O and subsurface Ne. Only a small amount of oxygen, estimated to be less than 2% of a monolayer, could not be removed.

The intensities of the diffracted beams as a function of incident-electron energy, or I–V curves, were recorded from digitized video images of the LEED screen. All of the measurements were performed with the electron beam incident normal to the surface at a sample temperature of 110 K. Normal incidence was determined by adjusting the position of the sample until the I–V curves of symmetry-related beams were equivalent.

The geometry of the bulk-terminated Be(11$\bar{2}$0) surface is illustrated in Fig. 1. The unit cell is nearly square (3.95 Å × 3.58 Å), and the surface is characterized by zig-zag chains which run parallel to the c-axis of the bulk (the [0001] direction). The zig-zag chains arise from the A-B-A-B stacking sequence of (0001) planes, as is evident from the side-view of the structure shown in Fig. 1b. These chains are analogous to the linear chains of the fcc (110) surface. Of importance for the present analysis is the existence of a glide plane oriented parallel to the [0001] direction, i.e. parallel to the zig-zag atomic chains. This glide plane symmetry leads to the extinction of the (0,n) reflexes for odd values of n. The extinction of the (0,n) reflexes at the reconstructed (1 × 3) surface indicates that the internal structure of the zig-zag chains is preserved by the reconstruction [20].

The bulk-terminated structure contains only one mirror plane, parallel to the [10$\bar{1}$0] direction. However, the diffraction patterns from the surface are consistent with mirror planes parallel to both the [10$\bar{1}$0] and [0001] directions. The apparent mirror symmetry with respect to the [0001] direc-

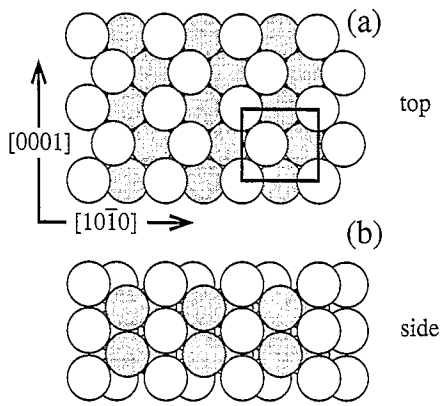

Fig. 1. (a) Top view and (b) side view of the bulk-terminated Be (11$\bar{2}$0) surface.

tion comes from incoherent diffraction from two possible domains. These domains arise from stacking faults in the A-B-A-B stacking of (0001) planes in the bulk, which give rise to mirror reflections of the crystal structure at the surface. Scattering from the two domains creates a diffraction pattern which appears to exhibit two perpendicular mirror planes.

The curve in Fig. 2 shows the diffracted intensity along a line parallel to the [10$\bar{1}$0] direction of the surface, and passing through the (n1) reflexes. Near the position of the (11) reflex, two fractional-order spots are observed at the (2/3,1) and (4/3,1) positions. As a function of incident energy, the intensity of these split spots oscillates out of phase with that of the (11) reflex. This behavior implies the existence of a well-ordered step array at the surface, with a terrace width of 1.5 bulk unit cells [20]. We have tested three possible structural models (shown in Fig. 3) which were used as input for the full dynamical calculations. All of the models preserve the zig-zag structure of the chains parallel to the [0001] direction, as is implied by the glide plane symmetry of the diffraction patterns. The (1 × 3) MR structure, favored by both the full dynamical calculation and the kinematic model, is shown in Fig. 3a. A related model, in which every third surface chain is moved to the bridge site formed by the remaining two chains, is depicted in Fig. 3b. This model corresponds to the creation of an array of (10$\bar{1}$0) microfacets (MF) at the surface. Lastly, a model based on the removal of two surface chains, or equivalently the addition of a single row (AR), is shown in Fig. 3c. In our analysis of the data, the calculated I–V curves from these trial structures were compared to the corresponding experimental curves. In the course of the analysis, the geometry of trial structures was relaxed to maximize the agreement between the experimental and calculated diffraction.

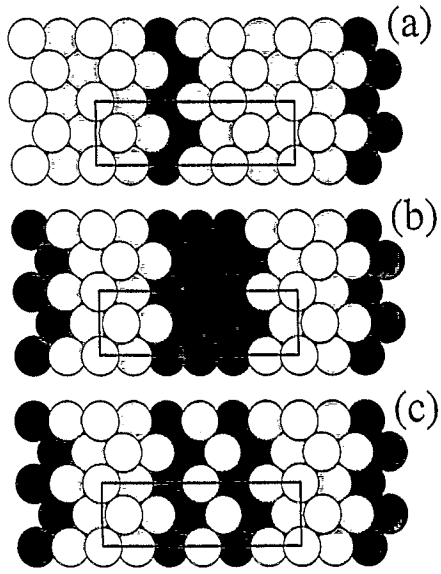

Fig. 3. Three models of the Be(11$\bar{2}$0)(1 × 3) reconstruction: (a) the missing-row model, (b) the micro-facet model, and (c) the added-row model. Atoms with a lighter shading are situated closer to the surface.

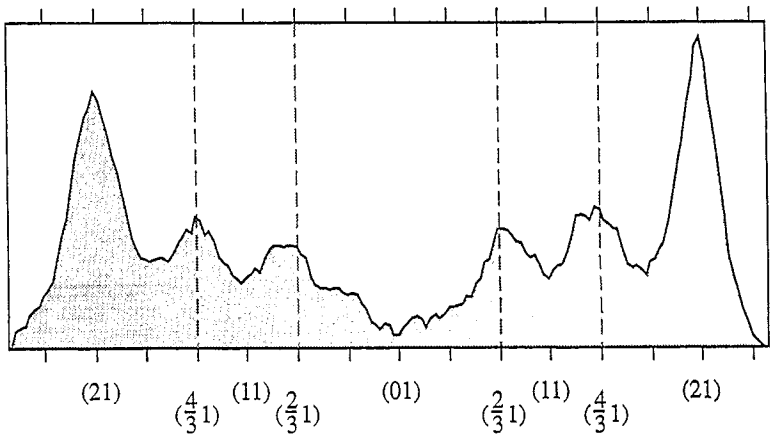

Fig. 2. Diffracted intensity as a function of momentum transfer parallel to the [10$\bar{1}$0] direction and passing through the (n1) reflexes. The incident-electron energy is 123 eV.

Because of the large dimensions of the reconstructed unit cell, it was not possible to separate the intensity of the split spots from that of the neighboring integer-order diffraction at higher incident-electron energies. Therefore, we have compared the sum of the measured intensities from the $(n,m-1/3)$, (n,m), and $(n,m+1/3)$ spots to the sum of the calculated intensities for these reflexes. We shall refer to this sum as beam (n,m), i.e. (11), (20), (02), (21), (12), (22), (30), (13), (32), (23), (40), (41), (04). The relative contribution of the fractional order spots versus the integer order spots was about 1:10 in the calculation. The data set which was used to determine the surface geometry is shown in Fig. 4, where the experimental I–V curves for 13 independent reflexes (solid lines) is compared over a total energy range of 2026 eV with the calculated I–V curves of the optimized (1×3) MR structure.

During the search for optimum agreement between experiment and calculation, the atomic positions of the surface atoms were relaxed. All relaxations consistent with the p2mg symmetry of the surface were applied to the top two layers of the surface. These include a possible buckling of the overlayer and a distortion of the zig-zag amplitude of the surface chains. Relaxation of the third and fourth layers normal to the surface was also considered. The reliability factors and optimized geometry for each of the trial structures are given in Table 1. The best agreement between calculation and experiment is found for the (1×3) MR structure, illustrated in Fig. 3a. The optimized geometry corresponds to a contraction of the first interlayer spacing, $\Delta d_{12}/d_0=(-14.9\pm3.1)\%$, and a small expansion of the second interlayer spacing, $\Delta d_{23}/d_0=(+5.3\pm3.7)\%$. The spacing between the third and fourth layer is almost bulk-like, with a

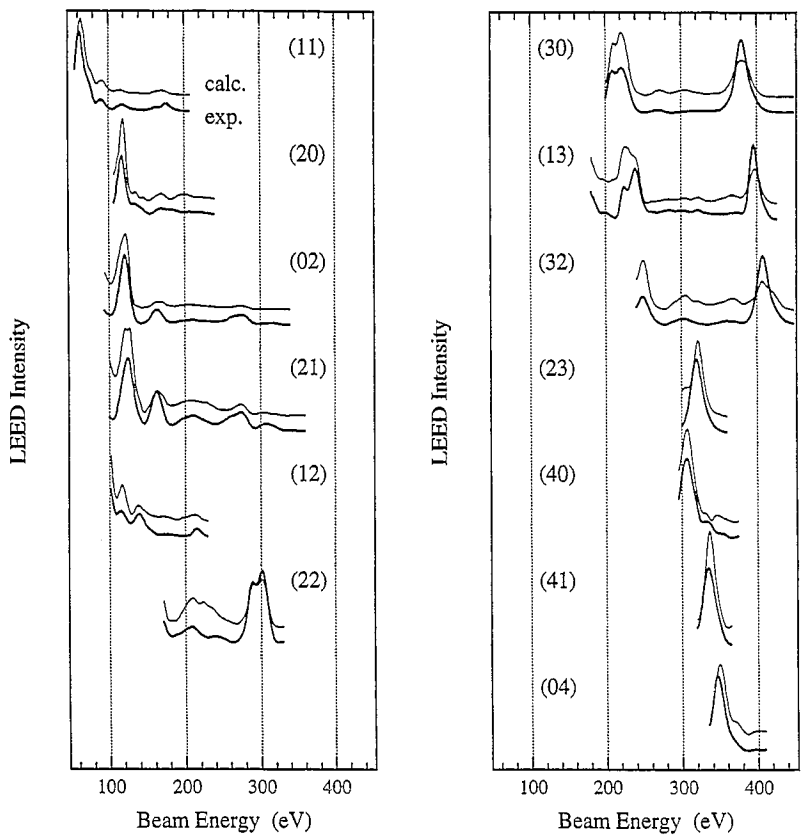

Fig. 4. Solid thick lines represent the experimental I–V curves and the upper thin curves are the theoretical curves for the optimized missing-row model.

Table 1
Geometrical parameters and the Pendry R-factors determined for the optimized trial structures

Trial structure	$\Delta d_{12}/d_0$ (%)	$\Delta d_{23}/d_0$ (%)	$\Delta d_{34}/d_0$ (%)	R_P
Missing row MR	-14.9 ± 3.1	$+5.3\pm3.7$	$+0.9\pm2.5$	0.212
Microfacets MF	-17.5	$+10.5$	-2.6	0.334
Added row AR	-15.8	$+1.8$	$+0.9$	0.359

slight expansion of $\Delta d_{34}/d_0=(+0.9\pm2.5)\%$. Relaxations parallel to the surface could not be unambiguously determined from the data. The real and imaginary parts of the optical potential were determined to be $V_{0r}=(-8.0+0.015(E-200))$ eV and $c=-7.0$ eV, respectively. The optimal surface Debye temperature was determined to be $\Theta_D^s=800$ K, which corresponds to a mean square displacement of $\langle u^2\rangle^s=0.0164$ Å^2.

The variation of R_P as a function of the first interlayer spacing is shown in Fig. 5. The lowest value of R_P reached is 0.212. With the total energy range of $\Delta E=2026$ eV, the difference by which the MR reconstruction is favored lies outside the variance of the R-factor

$$\sigma(R)=R_{\min}\sqrt{\frac{8|V_{0i}|}{\Delta E}}=0.212\sqrt{\frac{8|c|}{\Delta E}}=0.03,$$

and is therefore significant. This absolute value is slightly higher than the value of 0.180 calculated for the bulk-terminated Be(0001) surface [9], as well as the value of 0.175 calculated for the hydrogen-induced $(\sqrt{3}\times\sqrt{3})$R30° reconstruction of Be(0001) [26], but better than the R_P of 0.26 for Be(10$\bar{1}$0). We take this as a sign of poorer long-range order for this system. The angular width of the diffracted beams for the Be(11$\bar{2}$0) surface indicate that order perpendicular to the chains is significantly worse than order parallel to the chains. As is discussed in detail below, the calculated surface energies for (1×3) structures with zero, one, and two missing rows are very close. It is likely that perfect (1×3) periodicity parallel to the surface is interrupted by defects corresponding to additional or missing surface rows. To account

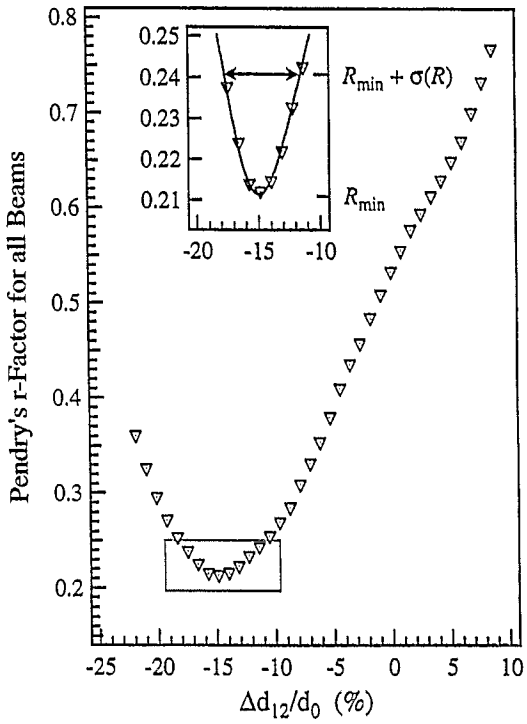

Fig. 5. A plot of the Pendry R-factor versus the first interlayer spacing. The insert shows the calculation of the error bars.

for this effect, we mixed optimized AR and BT domains of various ratios to the optimized MR structure by averaging the diffraction intensities before the comparison with the experimental curves was performed. However, this procedure did not lead to a significant improvement in the R-factor.

In order to understand the mechanism behind the MR reconstruction at the Be(11$\bar{2}$0) surface, we have compared our proposed surface structure to those calculated by Stumpf, who has performed fully relaxed first-principles total-energy calculations for a large number of possible surface configurations, including AR, MR, and MF structures [27]. Some general results can be drawn from these calculations. Structures which involve removal of atoms from the zig-zag chains are not energetically favored. That is, models possessing linear chains, or periodic vacancies within the chain, all have large surface energies (greater than 183 meV Å^{-2} for the models considered) [27]. This implies that the zig-zag chain is a stable unit, which is confirmed by the fact that the reconstruc-

tion maintains the glide plane symmetry of the bulk. Secondly, Stumpf finds that structures with missing or added chains have surface energies which are surprisingly close: BT 148 meV $Å^{-2}$, MR 149 meV $Å^{-2}$, MF 154 meV $Å^{-2}$ and AR 149 meV $Å^{-2}$ [27]. As the measured angular width of the diffracted beams indicates, the (1×3) MR surface may have defects of (1×3) cells with two or no missing rows. The influence of disorder on the surface stability is unknown, and is unlikely to be calculated because the surface cell required would contain a very large number of atoms.

Johansson et al. [28] have recently measured the surface core-level shifts (SCLS) at the Be $(11\bar{2}0)$ surface and found a single surface feature shifted to higher core-state binding energy (+0.41 eV). This value can also be compared to the results of the calculations of Stumpf [27], who computed the initial state contribution to the SCLSs for this surface. The BT and AR model would have SCLSs of −0.37 and −0.40 eV for one of their first two layers, which should be easily detectable in the experiment. Only the results for the MR model are consistent with the measurement: the atoms of the second layer would show a large SCLS of +0.48 eV. The peak from the first-layer atoms at −0.12 eV might be hidden in the rather broad peaks of the experiment.

Surprisingly, the first-principles calculations predict that the BT surface is the most stable configuration of the set of trial structures considered, for both unrelaxed and fully-relaxed geometries. This situation is in contrast with the results for Au(110) where, even for the unrelaxed surfaces, the MR geometry is favored [18]. Given the success of pseudopotential methods in predicting the structures of metal surfaces, the disagreement between theory and experiment in the present case is, perhaps, significant; LDA calculations for the Be(0001) [13] and Be$(10\bar{1}0)$ [29] surfaces agree well with the experimentally determined structure [8,9,12]. It may be that the corrugated geometry and low symmetry of the MR surface requires a more complicated treatment of exchange and correlation within the LDA formalism. Gradient corrections to the charge density might favor systems with a larger surface area, like the MR reconstruction. A more mundane source of discrepancy is the fact that the calculations are performed for a perfectly periodic lattice at 0 K, and that the experiments were carried out on crystals with steps, domains and defects. Given the small energy differences between the possible surface structures, entropy effects, steps or defects might stabilize the MR structure. A comparison to the phase stability of the alkali metals could give some insight in the importance of finite temperature effects. First-principles total-energy calculations for alkali metals [30] indicate that the energy differences between various possible structures is extremely small. Experimental evidence suggests that the equilibrium phases of these materials may be determined by the vibrational entropy of the lattice [31].

LEED data from the Be$(11\bar{2}0)$ surface indicates that the surface undergoes a (1×3) reconstruction for temperatures in the range 80–725 K. Analysis of the diffracted intensity, using both kinematic and multiple-scattering models, favors a missing-row structure in which every third chain of atoms in the bulk-terminated structure is removed. This conclusion is at odds with the first-principles total-energy calculations of Stumpf [27], which indicate that the bulk-terminated structure is favored over any of the reconstructed surfaces considered. However, in agreement with our experimental findings, the calculations show that the zig-zag chain structure is stable, and that defects in the form of missing or added chains are expected.

The discrepancy between the first-principles calculations and the experimental results serves to highlight the fact that the surface structure of Be $(11\bar{2}0)$ is an ideal test case for improvements upon current calculational schemes. The mechanism stabilizing the reconstruction is unknown, but must be different from that invoked at fcc (110) surfaces because Be possesses no occupied d-bands. The reconstruction of this surface is an indication that simple metal surfaces can exhibit complicated structural rearrangements at the surface which belie the simple picture of a free-electron metal. Indeed, even for the simple metals, it is now becoming clear that conceptually simple ideas about relaxation at surfaces, i.e. Smoluchowski charge smoothing [1], are of limited value in gaining insight into the equilibrium structure of surfaces.

Acknowledgements

We wish to thank Roland Stumpf and Harold Davis for many useful discussions and collaborations. We are also indebted to Stefan Müller and Klaus Heinz for supplying us with the Be phase shifts used in the LEED I–V calculation. This work was supported by the National Science Foundation under contract DMR-9510132. Part of this study was conducted at ORNL, managed by Lockheed Martin Energy Research Corporation for the US Department of Energy under contract number DE-AC05-96OR22464.

References

[1] R. Smoluchowski, Phys. Rev. 60 (1941) 661.
[2] L. Pauling, The Nature of the Chemical Bond, 3rd ed. (Cornell University Press, Ithaca, NY, 1960).
[3] R. Stumpf and M. Scheffler, Phys. Rev. B, to be published.
[4] A.P. Seitsonen, B. Hammer and M. Scheffler, Phys. Rev. B, to be published.
[5] P.J. Feibelman, Surf. Sci. 360 (1996) 297.
[6] M.W. Finnis and V. Heine, J. Phys. F 4 (1974) L37.
[7] R.A. Bartynski, E. Jensen, T. Gustafsson and E.W. Plummer, Phys. Rev. B 32 (1985) 1921.
[8] H.L. Davis, J.B. Hannon, K.B. Ray and E.W. Plummer, Phys. Rev. Lett. 68 (1992) 2632.
[9] K. Pohl, J.B. Hannon and E.W. Plummer, to be published.
[10] P.J. Feibelman, Phys. Rev. B 46 (1992) 2532.
[11] Ph. Hofmann, R. Stumpf, V.M. Silkin, E.V. Chulkov and E.W. Plummer, Surf. Sci., to be published.
[12] Ph. Hofmann, K. Pohl, R. Stumpf and E.W. Plummer, Phys. Rev. B, to be published.
[13] R. Stumpf and P.J. Feibelman, Phys. Rev. B 51 (1995) 13747.
[14] W. Moritz and D. Wolf, Surf. Sci. 88 (1979) L29.
[15] D.L. Adams, H.B. Nielsen, M.A. Van Hove and A. Ignatiev, Surf. Sci. 104 (1981) 47.
[16] C.M. Chan, M.A. Van Hove, W.H. Weinberg and E.D. Williams, Surf. Sci. 91 (1980) 440.
[17] C. Kittel, Introduction to Solid State Physics, 5th ed. (Wiley, New York, 1976) p. 74, Table 1.
[18] K.-M. Ho and K.P. Bohnen, Phys. Rev. Lett. 59 (1987) 1833.
[19] B.H. Lengsfield III, A.D. McLean, M. Yoshimine and B. Lui, J. Chem. Phys. 79 (1983) 1891.
[20] J.B. Hannon, E.W. Plummer, R.M. Wentzcovitch and P.K. Lam, Surf. Sci. 269 (1992) 7.
[21] M.A. Van Hove and S.Y. Tong, Surface Crystallography by LEED (Springer, Berlin, 1979).
[22] J.B. Pendry, Low Energy Electron Diffraction (Academic Press, London, 1974).
[23] S. Müller and K. Heinz, private communication.
[24] International Tables for X-Ray Crystallography (The Kynoch Press, Birmingham, 1962).
[25] J.B. Pendry, J. Phys. C 13 (1980) 937.
[26] K. Pohl, J.B. Hannon, D.B. Poker and E.W. Plummer, to be published.
[27] R. Stumpf, J.B. Hannon, P.J. Feibelman and E.W. Plummer, in: Electronic Surface and Interface States on Metallic Systems, Eds. E. Bertel and M. Donath (World Scientific, Singapore, 1995) p. 151.
[28] L.I. Johansson, H.I.P. Johansson, E. Lundgren, J.N. Andersen and R. Nyholm, Surf. Sci. 321 (1993) L219.
[29] R. Stumpf, private communication.
[30] A.Y. Liu and M.L. Cohen, Phys. Rev. B 44 (1991) 9678.
[31] S. Alexander and J. McTague, Phys. Rev. Lett. 41 (1978) 702;
[32] J.R. Morris and R.J. Gooding, Phys. Rev. Lett. 65 (1990) 1769.